Synthesis of unnatural α-*N*-linked glycopeptides with potential antifreeze activity

Cinzia Colombo,[1] Mattia Stucchi,[1] Chantelle J. Capicciotti [2], Robert N. Ben, [2] Anna Bernardi.[1]

[1] Universita' degli Studi di Milano, Dipartimento di Chimica, via Golgi 19, I-20133 Milano, Italy, [2] University of Ottawa, Department of Chemistry, Ottawa, ON K1N 6N5

The synthesis of neo-glycoconjugates has been gaining much attention in recent years due to the relevance of glycopeptides and glycoproteins in many biological processes.[1] Our group has been actively dedicating its efforts to the synthesis of α-*N*-linked glycosylamides and glycopeptides.[2,3] α-*N*-linked glycopeptides are unnatural molecules, since they display an α-linkage between the peptide side chain and the sugar moiety, unlike natural *N*-linked glycopeptides that connect the peptide to the glycan through a β-*N*-glycosidic bond. This novel type of peptide glycosylation could introduce structural modifications that can mimic and/or interfere with molecular recognition events.[4] Direct glycosylation of peptide chains is not viable for the synthesis of molecules with the α-*N*-linked configuration, since the corresponding α-glycosyl amines isomerise to the β-anomers. Only very recently N^{α}-Fmoc-protected glycosyl amino acids have been efficiently and stereoselectively synthesized and linearly incorporated into a peptide sequence. [3]

In the present paper these novel building blocks have been employed for the synthesis of complex structures that resemble antifreeze glycopeptides (Figure 1)**.**[5] These sequences were prepared using Fmoc solid-phase synthesis, experimenting with different conditions and also using microwave assisted solid-phase synthesis, in an effort to enhance the reactivity of our unnatural building block. The α-*N*-linked glycopeptides were obtained with modest yields, and their antifreeze properties were evaluated. Despite the fact that our compounds do not show significant antifreeze activity, this work constitutes the first attempt towards the synthesis of complex α-*N*-linked glycopeptides and has been useful to understand the behaviour, sometimes unexpected, of these molecules, in terms of reactivity and stability.

Keywords: α-*N*-linked glycopeptides, unnatural glycopeptides, antifreeze glycopeptides, microwave assisted synthesis, solid phase synthesis

Introduction:

Glycopeptides and glycoproteins are a family of biomolecules essential to many important biological processes including fertilization, immune defence, viral replication, parasitic infection, cell growth, cell-cell adhesion, degradation of blood clots, and inflammation.[1] Generally, oligosaccharides are attached to proteins mainly through the hydroxyl group of serine and threonine (*O*-glycans) and the amido group of asparagine (*N*-glycans). Natural *N*-linked glycopeptides are almost invariably β-linked. Therefore, the stereoselective synthesis of neo-glycoconjugates in the α-*N*-linked configuration has not been well explored, but is of great interest as a means of designing glycopeptide mimics with possible altered metabolic stability and novel physico-chemical properties. Several years ago Imperiali and Woods reported one case whereby the peptide conformation of an *N*-linked glycopeptide was found to depend on the α or β anomeric configuration of the appended glycan.[6] New data, however, has been lagging, mostly because of the lack of methods able to secure a viable synthesis of α-*N*-linked glycopeptides. This is what prompted us to establish appropriate methodologies for the access to this interesting class of novel glycoconjugates. Indeed, during the past few years, our laboratory has been actively exploring the synthesis and biological applications of such unnatural glycoconjugates and glycopeptides. [2,4,7,8] The convergent approach, which involves direct glycosylation of a pre-formed peptide chain, is precluded by the synthetic difficulties of α-*N*-glycosylation, since the corresponding α-glycosyl amines isomerise to the β-anomers. Hence, forced to employ α-*N*-linked glycosyl amino acids to be linearly incorporated into a peptide sequence, we initially dedicated our efforts to the development of an efficient stereoselective synthesis of N^{α}-Fmoc-protected glycosyl amino acids as suitable building blocks for solid-phase synthesis applications. Through the use of the DeShong methodology[9] and further elaborations, the N^{α}-Fmoc-protected galactopyranosyl-L-asparagine derivative **1** (**Scheme 1**) was obtained in good yields.[3] This novel building block finally allowed the synthesis of unnatural α-*N*-linked glycopeptides in a linear solid-phase peptide synthesis (SPPS) approach. In particular, we developed the synthesis of mimics of antifreeze glycopeptides, which contained repeating glycosylated tripeptide units of the general structure $(Ala\text{-}Asn(\alpha\text{-}N\text{-}Gal)\text{-}Ala)_n$ (**Figure 1a**). In nature, antifreeze glycopeptides (AFGPs) are mucin-like, peptide-based structures, composed of the repeating tripeptide unit $(Ala\text{-}Thr\text{-}Ala)_n$ in which the secondary hydroxyl group of the threonyl residue is glycosylated with the disaccharide β-D-Gal-(1→3)-α-D-GalNAc (**Figure 1b**).[10] These glycopeptides are present in polar fish blood serum and are essential to their survival as they prevent *in vivo* ice crystal growth.[11] AFGPs have the ability to irreversibly bind to the surface of ice crystals, thereby preventing further ice crystal growth through an adsorption-inhibition process. This results in a depression of the freezing point of the ice crystal (through the

Kelvin effect) relative to the melting point, an activity known as thermal hysteresis (TH) activity.[12] AFGPs also have the ability to inhibit the enthalpically driven process of ice recrystallization, an activity known as ice recrystallization inhibition (IRI) activity.[13,14] These remarkable molecules have potential applications in many area of agriculture, the frozen-food industry and in cryopreservation in which ice crystal growth is damaging.[15] Recently, *C*-linked AFGP mimics have been reported by the Ben group (**Figure 1c** and **1d)**.[13,16,17] These molecules were potent inhibitors of ice recrystallization but did not to possess thermal hysteresis activity. These *C*-linked derivatives were also found to protect embryonic liver cells from cryo-injury at millimolar concentration, increasing cell viability after cryopreservation.

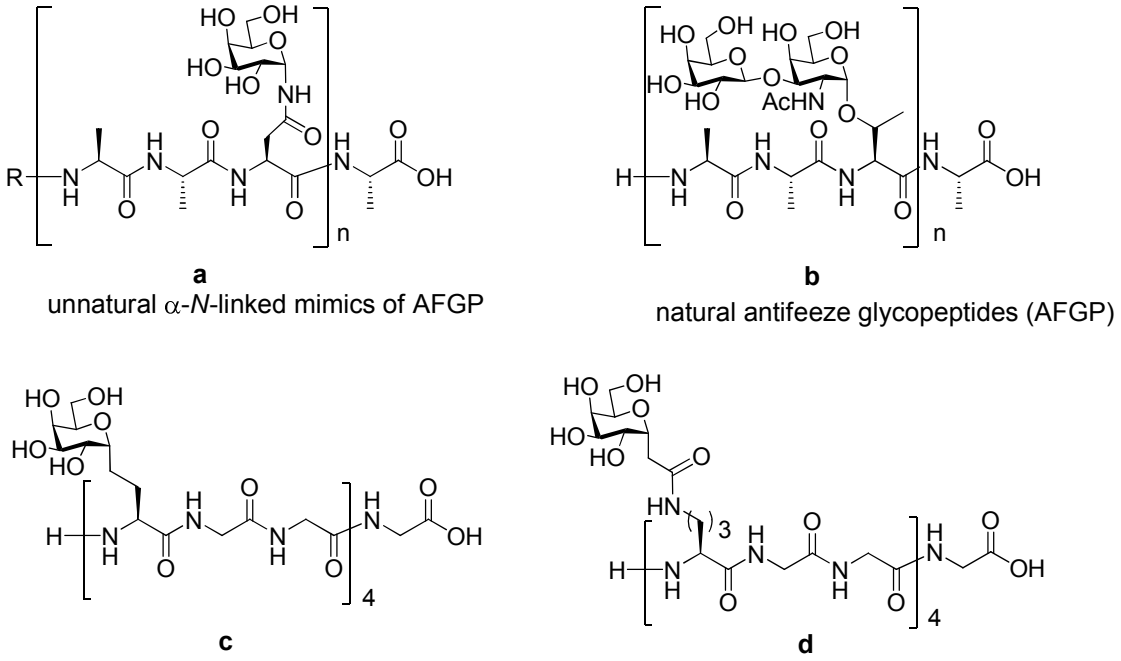

Figure 1. Unnatural α-*N*-linked glycopeptides **a**, natural AFGPs **b** and *C*-linked AFGP analogues **c** and **d**.

Hence, the design and the synthesis of antifreeze mimics appeared to be a challenging field, which could give opportunities to elucidate and predict the antifreeze activity of new molecules. For this purpose, we decided to synthesize glycopeptides of general structure **a** (**Figure 1**) that contain:

a) (Ala-Asn(α-N-Gal)-Ala) repeating units, with a hydrophobicity similar to the natural AFGPs **b**, and also display alanine residues;
b) A galactose moiety in place of a Gal-GalNAc disaccharide, as in the unnatural *C*-linked glycopeptides **c**-**d** reported by Ben;
c) An α-*N*-linked galactosyl asparagine in place of the Gal-GalNAc-threonyl residues of natural AFGPs **b**.

With the α-*N*-linked galactosyl amino acid **1** in hand, the synthesis of glycopeptides **2** and **3** was performed by Fmoc-SPPS using H-Ala preloaded 2-chlorotrityl resin (**Scheme 1**). The synthesis of **2** was performed at room temperature, using **1** and Fmoc-Ala-OH **4** as building blocks (**Scheme 1**).

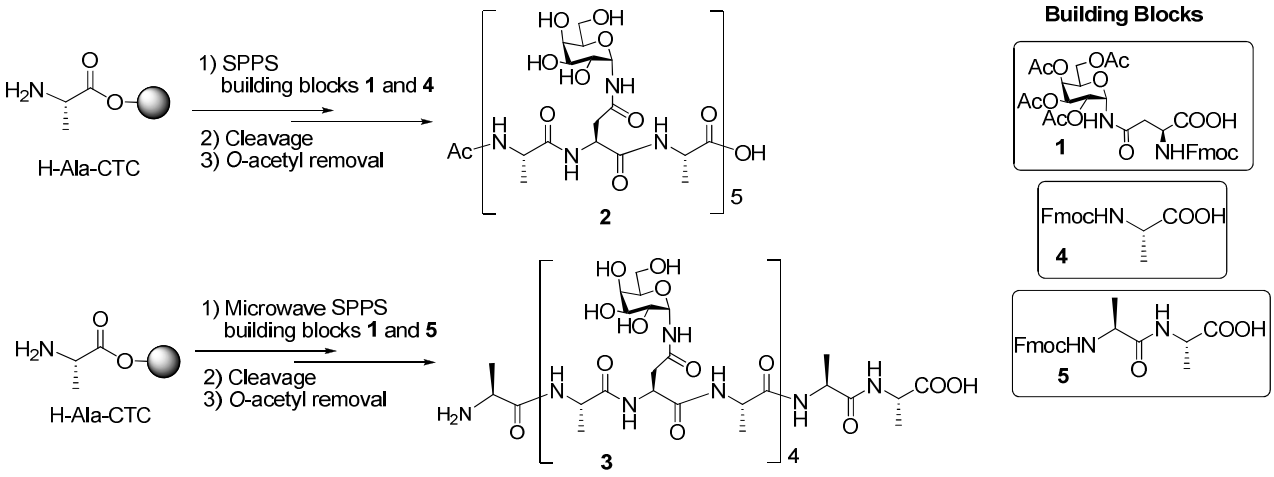

Scheme 1. Strategy for the synthesis of α-*N*-linked glycopeptides **2** and **3.**

The synthesis of glycopeptide **3**, which is structurally similar to **2** except it contains two alanine residues as spacers at the resin side and it lacks the *N*-terminal acetyl group, was performed using microwave (MW) assisted solid-phase synthesis using **1** and Fmoc-Ala-Ala-OH **5** as building blocks. The synthesis of these unnatural structures was difficult due to the low reactivity of the unnatural building block **1** in peptide coupling reactions. Methods for clean sugar deprotection and isolation of glycopeptides **2** and **3** have been identified, which allowed us to purify even rather heterogeneous mixtures of compounds. Finally, the antifreeze activity of the synthesized peptides was assessed; both the analogues **2** and **3** failed to demonstrate any significant TH activity or ice recrystallization inhibition (IRI) activity.

Methods / Experim:

Solvents were dried by standard procedures: *N*,*N*-diisopropylethylamine (DIPEA) was dried over calcium hydride, N,N-dimethylformamide (DMF) was dried with activated molecular sieves (3Å). H-Ala-2-chlorotrityl resin was purchased from Bachem. Solid phase reaction at room temperature were performed in Biotage Isolute column reservoirs (3mL, 6mL, 15 mL) using Heidolph Vibramax 110 shaker. Microwave-assisted solid phase synthesis was performed with a Biotage Initiator + SPWave apparatus, equipped with a variable vortex mixer (300-1300 rpm). The reactor was a proprietary 2 mL (700-1100 μL), 5ml (1600-3200 μL) or 10ml (3600-6400 μL) vial and the mixer was set at 1100 rpm. UV/Vis spectra were recorded on an Agilent 8453 instrument. ^{1}H and ^{13}C-NMR spectra were recorded at 400 MHz on a Bruker AVANCE-400 instrument. Mass spectra were obtained with a Bruker ion-trap Esquire 3000 apparatus (ESI ionization). Biotage® SNAP KP-C18-

HS cartridges were used for reverse phase chromatography, performed with a Biotage SP1 Flash purification system with a dual-wavelength detector (254 and 210 nm). HPLC chromatography was performed with a double Waters 515 pump coupled with a photodiode array detector Waters 996. A Phenomenex LUNA HILIC (5micron, 250x4.60 mm) was used for analytic HPLC chromatography. A Phenomenex LUNA HILIC (5micron, 250x10 mm) was used for semi-preparative HPLC chromatography. Absorbance was measured at 215nm. HPLC-MS analyses were perfomed with Agilent 1100 with quaternary pump, diode array detector, autosampler, thermostated column holder coupled with MS: Bruker ion-trap Esquire 3000 with ESI ionization. The HPLC column was a Waters Atlantis 50x4.6 mm, 3 µm.

Synthesis of α-*N*-linked glycopeptide 2

Glycopeptide **2** was assembled manually, using pre-loaded H-Ala-2-chlorotrityl resin (loading 0.4–0.9 mmol/g). The resin was shaken in DMF for 30 min prior to the synthesis. Compound **1** (**x** mmol) and PyBrop (1.5·**x** mmol) were dissolved in a solution of DMF at 0 °C. DIPEA (4·**x** mmol + mmol of resin) was added and the reagents were stirred at 0 °C for 15 min, then added to the resin (see **Table 1** for exact number of equivalents **x** used at each cycle). The reaction mixture was shaken for 8 h at room temperature. The cycle (activation of **1** with PyBrop and DIPEA at 0°C, then addition to the resin) was repeated and the reaction mixture was shaken overnight at room temperature. If another cycle was necessary, the mixture was shaken for 8 h. The resin was filtered and washed with DMF. Capping was performed with a 2 M Ac_2O solution in DMF (1h). After Fmoc removal under standard conditions (20% piperidine in DMF; 30 min twice), the resin was washed thoroughly with DMF to remove all traces of piperidine. Fmoc-Ala-OH **4** (5 eq) and HATU (5 eq) were dissolved in DMF (c = 0.2 M) at 0 °C. DIPEA (10 eq) was added and the reagents were stirred at 0 °C for 15 min, then added to the resin. The reaction mixture was shaken at room temperature for 2h. This procedure was repeated twice. The resin was filtered and washed with DMF. After capping and Fmoc removal, the coupling of an other Fmoc-Ala-OH residue **4** was performed in the same way. The entire sequence (compound **1**, compound **4** x 2) was repeated 4 times. After coupling of the last amino acid, the resin was washed thoroughly with DCM to eliminate DMF traces. Cleavage was performed with 1% TFA in DCM. After evaporation, the crude was dissolved in toluene and stripped at reduced pressure. The crude *O*-acetyl-glycopeptide **8** was purified by reverse phase chromatography: C-18 Biotage cartridge; eluants: H_2O/CH_3CN (0.1 % TFA); flux: 15ml/min; gradient: 5%→100% CH_3CN in 14 min. Pure *O*-acetyl-glycopeptide **8** was dissolved in a 4M solution of $MeNH_2$ in EtOH (c = 0.05M). The reaction mixture was stirred for 4 h then the solvent was evaporated at reduced pressure and stripped three times with methanol.

An ammonium bicarbonate solution (1M) in methanol was added and the mixture was stirred for 1h. The solvent was evaporated and the crude was purified by semi-preparative HILIC chromatography: eluant: CH_3CN:H_2O 7:3 (10 mM buffer at pH=7.5 with ammonium bicarbonate/formate); flux: 5ml/min; t_r = 12 min. ^{1}H NMR (400 MHz, D_2O, 25 °C): δ = 5.52 (d, J = 3.6 Hz, 5H, 1-H), 4.70 (m, 5H, α-H-Asn), 4.22-4.15 (m, 9H, α-H-Ala), 4.05-4.00 (m, 1H, α-H-Ala), 4.00-3.95 (m, 5H, 2-H), 3.95 (bs, 5H, 4-H), 3.87-3.71 (m, 5H, 3-H), 3.70–3.63 (m, 5H, 5-H), 3.58–3.64 (m, 10H, 6-H), 2.90-2.74 (m, 10H, β-H-Asn), 1.93 (d, 3H, NHAc), 1.32-1.24 (m, 30H, CH_3Ala) ppm. ^{13}C NMR (300 MHz, D_2O, 25 °C): 76.7 (C-1), 72.7 (C-5), 69.2 (C-3), 68.8 (C-4), 66.1 (C-2), 60.8 (C-6), 50.4 (α-C-Ala), 49.9 (α-C-Asn), 49.7 (α-C-Ala), 36.1, 36.2 (β-CH_2-Asn), 21.1 ($NHCH_3$), 16.5, 16.0 (CH_3Ala) ppm. LC-MS (ESI): m/z = 1098.8 $[M/2 +23+23]^{2+}$. MALDI-MS: m/z = 2175.7 $[M+23]^+$.

Microwave-assisted Synthesis of α-*N*-linked glycopeptide 3

Glycopeptide **3** was assembled using pre-loaded H-Ala-2-chlorotrityl resin (loading 0.4–0.9 mmol/g) with semi-automated microwave-assisted solid phase synthesis at 45°C.

Compound **5** (1.4 eq) and HATU (1.4 eq) were dissolved in DMF (c = 0.2 M) at 0 °C. DIPEA (2.8 eq) was added and the reagents were stirred at 0 °C for 15 min, then added to H-Ala-2-chlorotrityl resin, previously swollen in DMF. The reaction mixture was shaken for 20 min at 45°C with microwave irradiation, then the resin was filtered. Capping was performed twice with a 2 M Ac_2O, 0,5 M HOBt solution in DMF for 1h. After Fmoc removal (25% piperidine in DMF; 5 + 10 min), the resin was washed thoroughly with DMF to remove all traces of piperidine. Compound **1** (**x** mmol) and PyBrop (1.5·**x** mmol) were dissolved in a solution of DMF at 0 °C. DIPEA (4·**x** mmol + mmol of resin) was added and the reagents were stirred at 0 °C for 15 min, then added to the resin (see **Table 2** for exact number of equivalents **x** used at each cycle). The reaction mixture was shaken for 20 min at 45°C with microwave irradiation. The cycle (activation of **1** with PyBrop and DIPEA at 0°C, then addition to the resin, reaction at 45°C with microwave irradiation for 20 min) was repeated twice. The resin was filtered and washed with DMF. After capping and Fmoc removal, Fmoc-Ala-Ala-OH **5** (5 eq), prectivated for 15 min at 0 °C with HATU (5 eq) and DIPEA (10 eq) in DMF (c = 0.25 M), was added to the resin. The reaction mixture was shaken at 45°C under microwave irradiation for 20 min, then the resin was filtered and the cycle (activation of **5** with HATU and DIPEA at 0°C, then addition to the resin) was repeated once again. After 20min of reaction at 45°C MW, the resin was filtered and washed with DMF. Capping and Fmoc-deprotection were performed as previously described. The sequence of couplings of compound **1** and compound **5** was repeated 3 times. After coupling of the last amino acid, the resin was washed

thoroughly with DCM to eliminate DMF traces. A solution 30% HFIP in DCM (2ml) was used for the cleavage. After evaporation, the crude was repeatedly dissolved in toluene and stripped at reduced pressure. Crude compound **12** was purified on reverse phase chromatography: C-18 Biotage cartridge; eluants: H_2O/CH_3CN; flux: 15ml/min; gradient: 5-60% acetonitrile in 14 min, 60-100% in 4 min. Pure compound **12** was then dissolved in a 4M $MeNH_2$-EtOH solution (c = 0.05M). The reaction mixture was stirred for 5 h and a white solid precipitated. The heterogeneous solution was centrifuged and the solution was removed. Repeating twice the operation with 3:1 ethanol/diethyl ether solution afforded the desired compound **3**, which was lyophilized. ^{1}H NMR (400 MHz, D_2O 5mM NH_4COO pH=5.25, 25 °C): δ = 5.63 (d, J = 5.3 Hz, 4H, 1-H), 4.75 (m, 4H, α-H-Asn), 4.37-4.12 (m, 11H, α-H-Ala), 4.09-4.04 (m, 4H, 2-H), 4.01 (d, J = 3.2 Hz, 4H, 4-H), 3.87-3.82 (m, 4H, 3-H), 3.80-3.76 (m, 4H, 5-H), 3.74-3.68 (m, 8H, 6-H), 3.06-2.83 (m, 8H, β-H-Asn), 1.60–1.53 (m, 3H, CH_3Ala), 1.47–1.32 (m, 30H, CH_3Ala) ppm. ^{13}C NMR (400 MHz, D_2O 5mM NH_4COO pH=5.25, 25 °C): δ = 76.96 (C-1), 72.02 (C-5), 69.49 (C-3), 68.92(C-4), 66.38 (C-2), 61.16 (C-6), 49.87 (α-C-Ala), 36.40 (β-CH_2-Asn), 16.61 (CH_3-Ala) ppm. LC-MS (ESI): m/z = 1905.8 $[M+1]^+$.

Thermal Hysteresis (TH) Assay

Nanoliter osmometry was performed using a Clifton nanoliter osmometer (Clifton Technical Physics, Hartford, NY) as described by Chakrabartty and Hew.[18] All measurements were performed in doubly distilled water. Ice crystal morphology was observed through a Leitz compound microscope equipped with an Olympus 20× (infinity-corrected) objective, a Leitz Periplan 32× photo eyepiece, and a Hitachi KPM2U CCD camera connected to a Toshiba MV13K1 TV/VCR system. Still images were captured directly using a Nikon CoolPix digital camera.

Ice Recrystallization Inhibition (IRI) Assay

Sample analysis for IRI activity was performed using the "splat cooling" method as previously described.[19] In this method, the analyte was dissolved in a phosphate buffered saline (PBS) solution and a 10 μL droplet of this solution was dropped from a micropipette through a two meter high plastic tube (10 cm in diameter) onto a block of polished aluminum precooled to approximately -80 °C. The droplet froze instantly on the polished aluminum block and was approximately 1 cm in diameter and 20 μm thick. This wafer was then carefully removed from the surface of the block and transferred to a cryostage held at -6.4 °C for annealing. After a period of 30 min, the wafer was photographed between crossed polarizing filters using a digital camera (Nikon CoolPix 5000) fitted to the microscope. A total of three images were taken from each wafer. During flash freezing, ice

crystals spontaneously nucleated from the supercooled solution. These initial crystals were relatively homogeneous in size and quite small. During the annealing cycle, recrystallization occurred, resulting in a dramatic increase in ice crystal size. A quantitative measure of the difference in recrystallization inhibition of two compounds is the difference in the ice crystal size distribution. Image analysis of the ice wafers was performed using a novel domain recognition software (DRS) program.[20] This processing employed the Microsoft Windows Graphical User Interface to allow a user to visually demarcate and store the vertices of ice domains in a digital micrograph. The data was then used to calculate the domain areas. All data was plotted and analyzed using Microsoft Excel. The mean grain (or ice crystal) size (MGS) of the sample was compared to the MGS of the control PBS solution for that same day of testing. IRI activity is reported as the percentage of the MGS (% MGS) relative to the PBS control, and the % MGS for each sample was plotted along with its standard error of the mean. Small percentages represent a small MGS, which is indicative of more potent IRI activity.

Results and Discussion:

The synthesis of glycopeptides **2** and **3** was performed employing the unnatural α-*N*-linked galactosyl building block **1** in a linear assembly strategy. The synthesis and an optimization of the coupling conditions of **1** were reported previously.[3] It was observed that during the activation at the C-terminus with almost all the commonly used coupling agents (HOBT, HBTU, HOAT, HATU), **1** undergoes a side reaction resulting in a consistent formation of aspartimide **7** through the intermediate **6**. This side reaction was found to be favoured by basic conditions and may result from a rather high acidity of the anomeric N-H group.

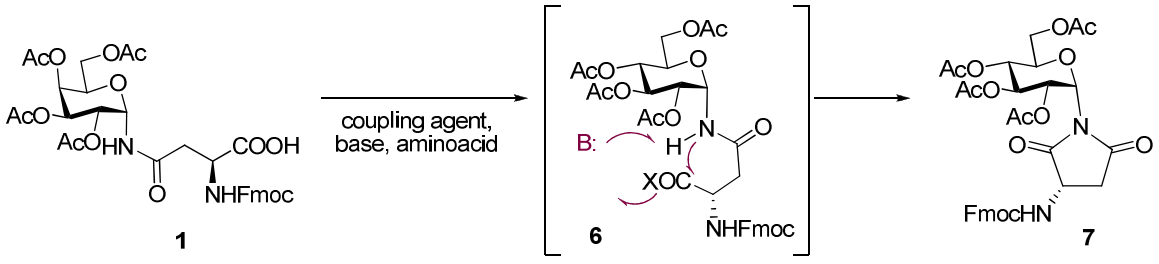

Scheme 2. General scheme for aspartimide formation from activation of α-*N*-linked galactosyl building block **1**.

In order to suppress aspartimide formation and to optimize the coupling conditions, various reagents were screened and only bromo-tris-pyrrolidino phosphonium hexafluorophosphate (PyBrop) was found to consistently increase the yield of the desired coupling reaction and decrease aspartimide formation.[3] Taking this into consideration, conditions for the solid phase synthesis of *O*-acetyl-glycopeptide **8** (**Scheme 3**) were explored. The general procedure was based essentially on a repeating sequence, which consisted in coupling the Fmoc protected α-galactosyl amino acid **1**,

using PyBrop activation, followed by coupling of two Fmoc-alanine residues **4**, using HATU activation (**Scheme 3**). The sequence was cycled up to 5 repeats. The solid-phase synthesis was performed on a H-Ala-Chlorotrityl resin, which is commercially available with a medium loading of 0.4-0.9 mmol/g. In the first coupling, the amount of the galactosyl amino acid **1** was adjusted to obtain a standard loading of 0.5 mmol/g, as established spectroscopically after standard Fmoc removal.

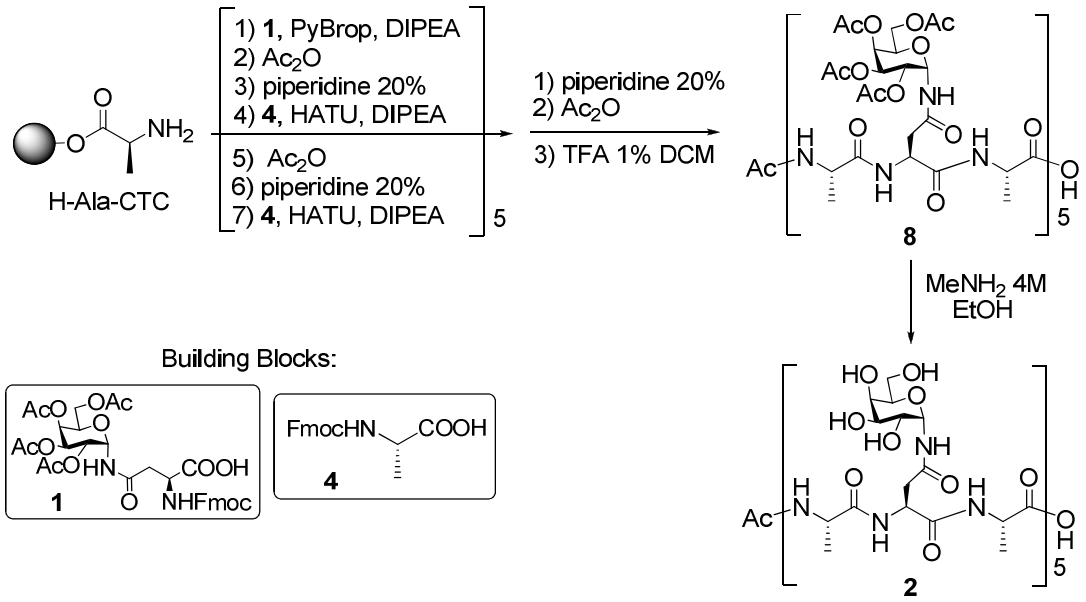

Scheme 3.Synthesis of glycopeptide **2**.

Coupling reactions with Fmoc-Ala-OH **4** were uneventful and were found to occur quantitatively when performed with 5 equivalents of **4** (c = 0.2 M in DMF) in 2h, for two cycles. Critical steps were instead those involving the galactosyl amino acid **1**, which reacted slowly and in relative low yields (**Scheme 2**). Consequently, the reaction time for galactosyl-asparagine couplings was extended and double or triple coupling cycles were performed. The optimized reaction conditions for each repeat are shown in **Table 1**.

Table 1. Reaction conditions for the coupling of galactosyl asparagine **1** at room temperature.

Entry	Repeat (n) [a]	Equivalents of **1 (x)**	Cycles	Reaction time (h)	[M] in DMF	Yield(%) [b]
1	1	1.5	1	8	0.1	- [c]
2	2	1.5	2	8 + 12	0.1	80
3	3	2	2	8 + 12	0.15	83
4	4	2	3	8 + 12 + 8	0.15	80
5	5	3	3	8 + 12 + 8	0.15	90

[a] Identifies the position of the coupled residue. [b] Yield determined by UV spectroscopy after Fmoc-removal. [c] First amino acid loaded on the resin (loading = 0.5 mmol/g).

Completion of the coupling step is indeed critical and the efficiency is deeply dependent on concentration, equivalent used, number of cycles and length of the sequence. It could be noted that more equivalents and more cycles are required for the attachment of **1** in the third, fourth and fifth repeats (**Table 1**). After deprotection of the Fmoc-group from the last alanine residue and acetylation, the peptide was cleaved from the resin with 1% TFA in DCM. The desired target **8** was purified by reverse phase C18 chromatography (H_2O/ CH_3CN 0.1% TFA) to remove some of the truncated sequences. Partial deacetylation occurred during chromatography. The isolated fractions were subjected to *O*-acetyl removal with a 4M solution of $MeNH_2$ in EtOH. [21] These conditions had to be carefully established, because of the instability of α-*N*-linked glycosyl amides to acidic and basic conditions (**Scheme 4**). *O*-acetyl deprotection with classical Zemplen reaction (catalytic MeONa in MeOH, followed by quenching with the sulfonic resin IRA 120 H^+) led to formation of the furanose glycopeptides **11** (10%), deriving from the opening and reclosure of the pyranose ring. Deacetylation with K_2CO_3 in MeOH (pH 8.5), followed by IRA 120 H^+ quench, also afforded ca 10% of furanose forms (**Scheme 4**). Finally we found that a 4M solution of $MeNH_2$ in EtOH afforded clean deprotection (**Scheme 4**). Excess $MeNH_2$ and most of the AcNHMe could be removed by evaporation. Under these conditions, glycopeptide **2** was isolated and purified by semi-preparative hydrophilic interaction liquid chromatography (HILIC)[22] (eluant: CH_3CN:H_2O 7:3, 10 mM buffer at pH=7.5 with ammonium bicarbonate/formate) with an overall yield of 6%.

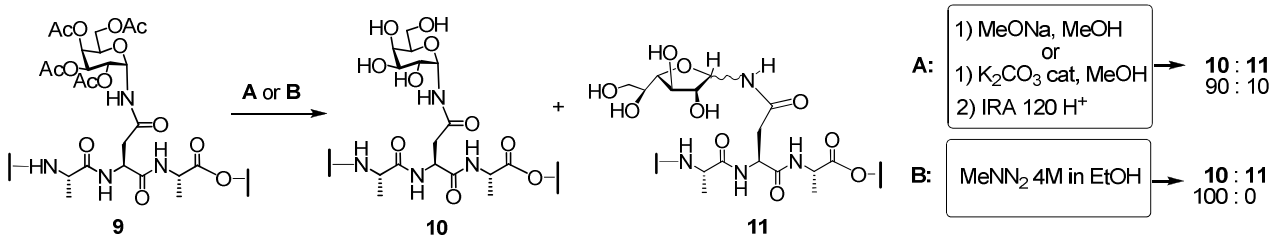

Scheme 4. Deprotection experiments for α -*N*-linked galactosyl peptides of general structures **9**

In general, α-*N*-linked galactosyl peptides of general structure **10** were found to be stable in water solution in a limited range of pH ($4 \leq pH \leq 9$).

To improve on the synthesis described above, we planned to reduce the number of steps in the synthesis of **3** using the Fmoc-Ala-Ala-OH building block **5**,[23] and to use microwave irradiation with the aim of accelerating the coupling reaction and increasing the coupling yields of **1** (**Scheme 5**). Since 2-chlorotrityl polystirenic resin is unstable at high temperature (>50°C) due to the trityl moiety, microwave-assisted couplings were run at 45°C. The procedures used are described in **Scheme 5** and the yields of galactosyl amino acid **1** coupling reactions are shown for each repeat in **Table 2**.

Table 2. Coupling of galactosyl asparagine **1** with microwave at 45°C.

Entry	Repeat (n) [a]	Equivalents of **1 (x)**	Cycles	Reaction time (min)	[M] in DMF	Yield(%) [b]
1	1	3	3	20min/cycle	0,37	95
2	2	3	3	20min/cycle	0,37	72
3	3	3	3	20min/cycle	0,2	64
4	4	3	3	20min/cycle	0,2	51

[a] Identifies the position of the coupled residue. [b] Yield determined by UV spectroscopy after Fmoc-removal.

Compared to **2,** glycopeptide **3** presents two main differences: it displays a free amine at the *N*-terminus, which may be beneficial for antifreeze activity, and it contains two additional alanine residues at the C-terminal side, spacing the resin from the glycopeptide with the scope of reducing the steric effects during the reaction of the first galactosyl amino acid.

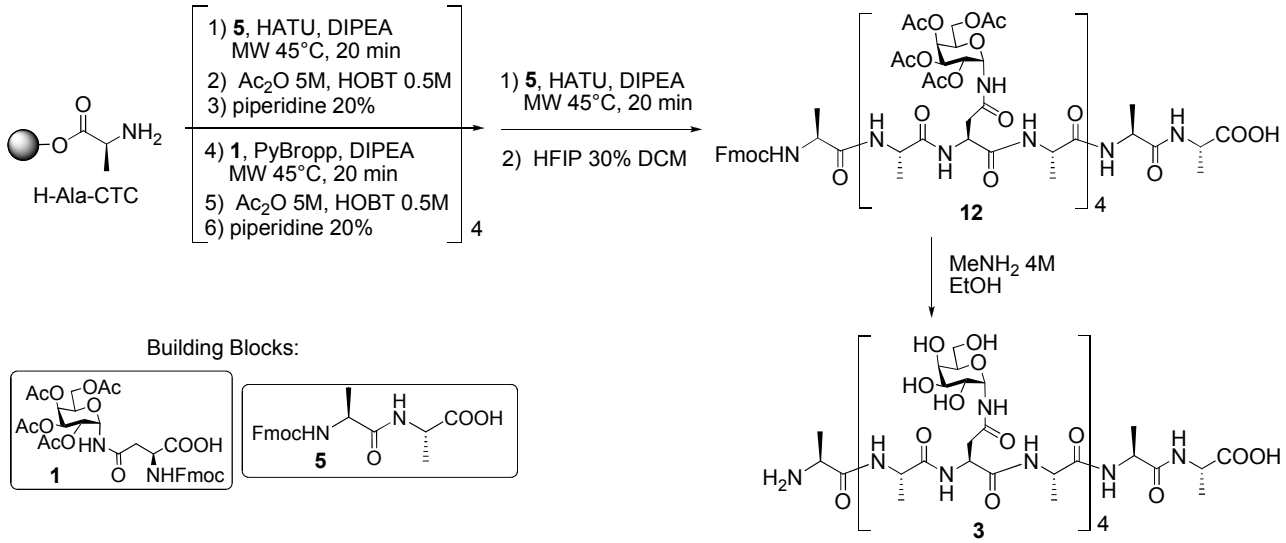

Scheme 5. Synthesis of glycopeptide **3**.

MW acceleration worked well for coupling of the first unit of **1**, bringing the yields up to 95%. However after the first repeat, the yields of the MW-assisted process were actually lower than those obtained at room temperature (compare **Table 1** and **Table 2**). Nonetheless, a remarkable benefit was observed in terms of reaction time (20 min versus 8-12h). Cleavage from the resins with 30% HFIP in CH_2Cl_2) followed by reverse phase chromatography (eluants: H_2O/CH_3CN) allowed to isolate **12**, *N*-Fmoc-protected, from the other truncated sequences and without *O*-deacetylation of the sugar. Simultaneous deacetylation and Fmoc removal were obtained with a 4M solution of $MeNH_2$ in EtOH. Pure glycopeptide **3** precipitated from the reaction mixture and was isolated by centrifugation with an overall yield of 7%.

Also for the synthesis of glycopeptide **3**, the major limitation resulted from the low reactivity of the glycosyl amino acid **1**. Further experiments were performed to improve the modest coupling yields,

including the use of different solvents, resins, activation conditions and bases, but none of these attempts gave better results.

Glycopeptides **2** and **3** were finally evaluated as possible antifreeze compounds. Both thermal hysteresis (TH) (**Figure 2**) and ice recrystallization inhibition (IRI) activities (**Figure 3**) were assessed. Both the compounds were dissolved in water and assessed for thermal hysteresis (TH) activity using nanolitre osmometry (**Figure 2**). Compound **2** was rather insoluble at 10 mg/mL and at 5 mg/mL and could only be tested at 3 mg/mL. Compound **3** was tested at 10 mg/mL. No TH activity or dynamic ice shaping capabilities was observed for either derivative, indicating these compounds were unable to bind to ice.

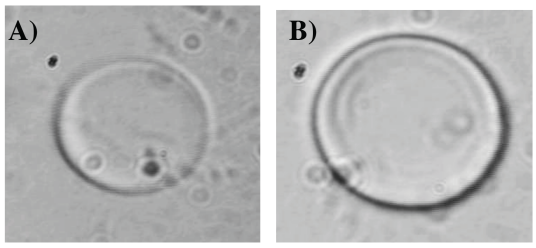

Figure 2. Ice crystal morphology in the presence of: A) α-*N*-linked glycopeptide **2** (3 mg/mL); B) α-*N*-linked glycopeptide **3** (10 mg/mL).

The IRI activity of compounds **2** and **3** are shown in **Figure 3**. In these measurements, native AFGP-8 was used as a positive control for IRI activity, while phosphate buffered saline (PBS) represented a negative control.[24] IRI activity is represented as the mean grain size ratio between the glycopeptide tested and the PBS control, thus the vertical axis in **Figure 3** represents this percent mean grain size (% MGS) ratio. Larger values (% MGS) thus indicate larger ice crystals and less inhibition of ice recrystallization. At a concentration of 5.5 μM, native AFGP-8 has potent IRI activity (**Figure 3**). However, glycopeptide **2** exhibited no IRI activity at this concentration and, in fact, had the same activity of the negative PBS control. At 1 mM both glycopeptides **2** and **3** show nearly the same negligible IRI activity. While at 5.5 mM glycopeptide **3** did exhibit the ability to inhibit ice recrystallization, its activity was activity 2-3 times lower than AFGP-8 at a significantly higher concentration. The IRI activity of glycopeptide **2** could not be measured at 5.5 mM due to solubility problems. In general, it can be concluded that **3** has no relevant IRI activity, despite the absence of *N*-Ac protecting group.

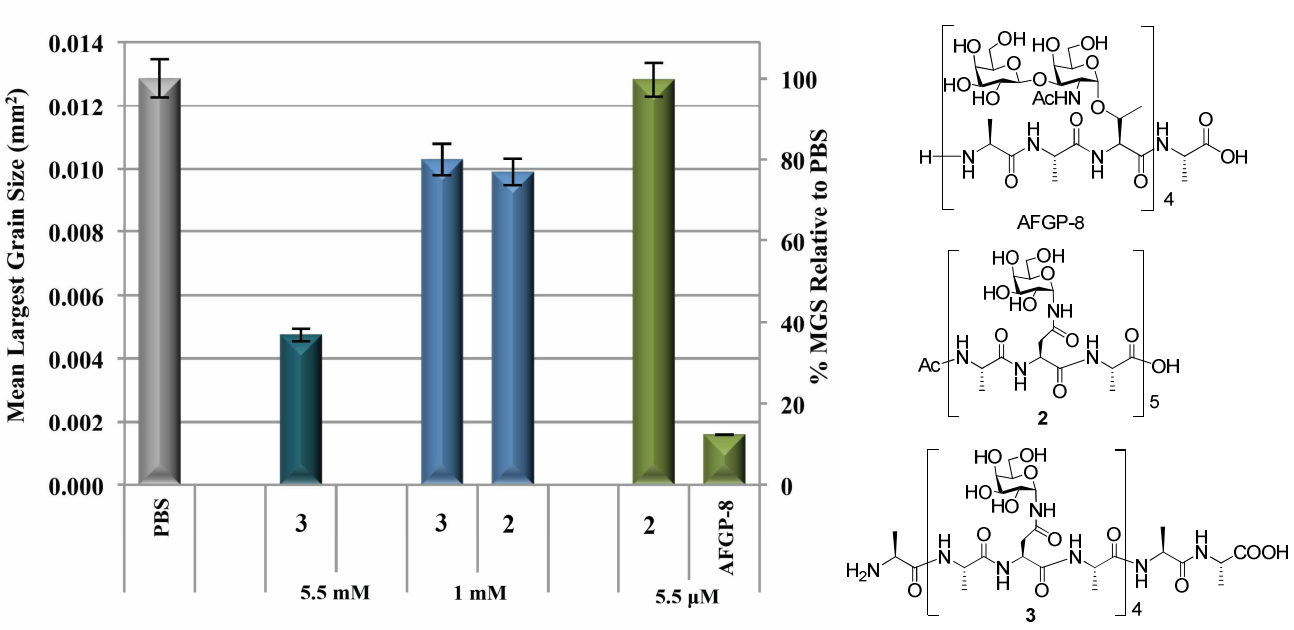

Figure 3. IRI activity of α-*N*-linked glycopeptides **2** and **3** assayed at the indicated concentrations. The % MGS (mean grain size) of ice crystals relative to PBS control is shown for each glycopeptide. PBS is used as a negative control for IRI activity and AFGP-8 is used as a positive control for IRI activity.

Conclusions:

This paper has described the synthesis of two unnatural α-*N*-linked galactosyl peptides **2** and **3** that resemble the structure of antifreeze glycopeptides. Although glycopeptides **2** and **3** do not possess any significant antifreeze property, this work represents the first attempt for the synthesis of unnatural α-*N*-linked glycopeptides. The major problems towards the synthesis of such structures were observed in the coupling reactions of the α-*N*-galactosyl asparagine building block **1**. This drawback was aggravated by the modular structure of the sequence selected, which contains multiple copies of the glycosyl amino acid. Aspartimide formation upon activation of **1** is not completely avoidable, although the use of PyBrop allows us to control the extent of this side reaction. Furthermore, microwave-assisted methodology did not improve the coupling yields, even if it allows a drastic reduction of coupling reaction times. Another obstacle was represented by the selection of conditions for *O*-acetyl removal at the sugar moiety, the general last step to obtain glycopeptides. Commonly used methods turned out to be harmful for our targets, since side reactions resulted in ring opening and contraction of the sugar and it was established that α-*N*-linked glycopeptides, when unprotected at the sugar moieties, must be handled in a limited range of pH (4≤ pH ≤9). Nonetheless, α-*N*-linked glycopeptides containing up to 15 residues and 5 copies of galactosyl asparagine have been synthesized. The methods developed here are expected to be

suitable for the synthesis of other α-*N*-linked glycopeptides, including α-*N*-glycosylated building blocks in other less challenging sequences.

Acknowledgements: This research was supported by funding from the University of Milan. C. J. C thanks Canadian Blood Services (CBS) for a GFP award.

References

[1] D. P. Gamblin, E. M. Scanlan, B. G. Davis, *Chem. Rev.* **2009**, *109*, 131-163.

[2] a) F. Nisic, A. Bernardi, *Carbohydr. Res.* **2011**, 346, 465-71.

[3] C. Colombo, A. Bernardi, *Eur. J. Org. Chem.* **2011**, 3911–3919.

[4] F. Marcelo, F. J. Cañada, S. André, C. Colombo, F. Doro, H. J. Gabius, A. Bernardi, J. Jiménez-Barbero. *Organic & Biomolecular Chemistry* 2012, DOI: 10.1039/C2OB07135E.

[5] a) Garner, J.; Harding, M. M. *ChemBioChem* **2010**, *11* 2489-2498. b) Leclere, M; Kwok, K. B.; Luke K. W.; Allan, D. S.; Ben, R. N. *Bioconjugate Chem.* **2011**, *22*, 1804-1810.

[6] Bosques, C. J.; Tschampel, S. M.; Woods, R.; Imperiali, B. *J. Am. Chem. Soc.* **2004**, *126*, 8421-8425

[7] Timpano, G.; Tabarani, G.; Anderluh, M.I.; Invernizzi, D.; Vasile, F.; Potenza, D.; Nieto, P.M.; Rojo, J.; Fieschi, F.; Bernardi, A. *ChemBioChem* **2008**, *9*, 1921-1930.

[8] Andreini, M.; Anderluh, MI.; Audfray, A.; Bernardi, A.; Imberty, A. *Carb. Res.* **2010**, *345*, 1400-1407.

[9] F. Damkaci, P. DeShong, *J. Am. Chem. Soc.* **2003**, *125*, 4408-4409.

[10] A. L. DeVries, S. K. Komatsu, R. E. Feeney, *J.Biol.Chem.***1970**, *245*, 2901.

[11] A. L. DeVries, D. E. Wohlschlag, *Science* **1969**, *163*, 1073.

[12] a) J. A. Raymond, A. L. DeVries, *Proc. Natl. Acad. Sci. USA* **1977**, *74*, 2589; b) C. A. Knight, C. C. Cheng, A. L. DeVries, *Biophys. J.* **1991**, *59*, 409; c) C. A. Knight, E. Driggers, A. L. DeVries, *Biophys. J.* **1993**, *64*, 252; d) C. A. Knight, A. L. DeVries, *J. Cryst. Growth* **1994**, *143*, 301; e) P. W. Wilson, *Cryo Lett.* **1993**, *14*, 31.

[13] Tam, R. Y.; Rowley, C. N.; Petrov, I.; Zhang, T.; Afagh, N. A.; Woo, T. K.; Ben R. N. *J. Am. Chem. Soc* **2009**, *131*, 15745–15753.

[14] Garner, J.; Harding, M. M. *ChemBioChem* **2010**, *11* 2489-2498.

[15] Wang, J.-H. *Cryobiology* **2000**, *41*, 1–9.

[16] Leclere, M.; Kwok, K. B.; Luke K. W.; Allan, D. S.; Ben, R. N. *Bioconjugate Chem.* **2011**, *22*, 1804-1810.

[17] Colombo C. PhD Thesis, Universita' di Milano, **2010-2011.**

[18] Chakrabartty, A.; Hew, C. L. *Eur. J. Biochem.* **1991**, *202*, 1057-1063.

[19] Knight, C. A.; Hallett, J.; DeVries, A. L. *Cryobiology* **1988**, *25*, 55-60.

[20] Jackman, J.; Noestheden, M.; Moffat, D.; Pezacki, J. P.; Findlay, S.; Ben, R. N. *Biochem. Biophys. Res. Commun.* **2007**, *354*, 340-344.

[21] Drenichev, M. S.; Kulikova, I: V.; Bobkov, G. V.; Tararov, V, I; Mikhailov, S. N. *Synthesis* **2010**, *22*, 3827-3834.

[22] Dejaegher, B.; Heyden, Y. V. *J. Sep. Sci.* **2010**, *33*, 698-715.

[23] Zhang, Y.; Gu, H.; Yang, Z.; Xu B. *J. Am. Chem. Soc.* **2003**, *125*, 13680-13681.

[24] a) Czechura, P.; Tam, R. Y.; Murphy, A. V.; Dimitrijevic, E.; Ben, R. N., *J. Am. Chem. Soc.*, **2008**, *130*, 2928–2929. b) Liu, S.; Ben, R. N., *Org. Lett.*, **2005**, *7*, 2385–2388.